
Generative Semantic Communication: Diffusion Models Beyond Bit Recovery

Eleonora Grassucci, Sergio Barbarossa, Danilo Comminiello

Department of Information Engineering, Electronics, and Telecommunication (DIET)

Sapienza University of Rome

Via Eudossiana 18, 00182, Rome, Italy

{eleonora.grassucci,sergio.barbarossa,danilo.comminiello}@uniroma1.it

Abstract

Semantic communication is expected to be one of the cores of next-generation AI-based communications. One of the possibilities offered by semantic communication is the capability to regenerate, at the destination side, images or videos semantically equivalent to the transmitted ones, without necessarily recovering the transmitted sequence of bits. The current solutions still lack the ability to build complex scenes from the received partial information. Clearly, there is an unmet need to balance the effectiveness of generation methods and the complexity of the transmitted information, possibly taking into account the goal of communication. In this paper, we aim to bridge this gap by proposing a novel generative diffusion-guided framework for semantic communication that leverages the strong abilities of diffusion models in synthesizing multimedia content while preserving semantic features. We reduce bandwidth usage by sending highly-compressed semantic information only. Then, the diffusion model learns to synthesize semantic-consistent scenes through spatially-adaptive normalizations from such denoised semantic information. We prove, through an in-depth assessment of multiple scenarios, that our method outperforms existing solutions in generating high-quality images with preserved semantic information even in cases where the received content is significantly degraded. More specifically, our results show that objects, locations, and depths are still recognizable even in the presence of extremely noisy conditions of the communication channel. The code is available at <https://github.com/ispamm/GESCO>.

1 Introduction

The next sixth generation (6G) of wireless networks is expected to bring a radical change in thinking and developing communication systems [1]. One promising aspect of semantic communication lies in its potential to reconstruct content that is semantically equivalent to the transmitted one, without necessarily requiring the recovery of the bits used to encode that content. This change of perspective may allow the receiver to make the proper decisions directly linked to its goal at the right time, even though the bits of the received message are corrupted by any channel adverse condition[2]. Recovering the right transmitted content can also be directly linked to the goal of communication. Suppose the explanatory scenario of a vehicle transmitting visual information about the street. The crucial information is to correctly detect the presence of pedestrians, their positions, and their distance, which is the semantic knowledge, rather than recovering bits and carrying out a pixel-wise reconstruction of the colors or of the surrounding buildings.

Nevertheless, the existing solutions in the field continue to grapple with various challenges, thereby hindering their ability to deliver optimal results. One prominent issue is the lack of capacity in building complex scenes from the received information that may be corrupted or incomplete. Existing

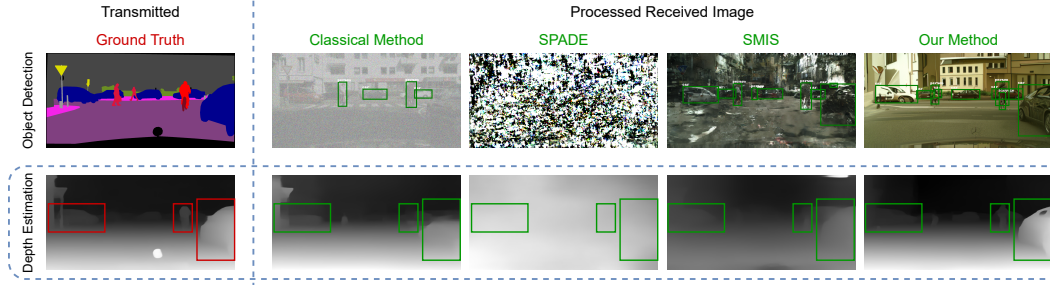


Figure 1: Synthesized images from the transmitted semantics with $\text{PSNR} = 10$ for the classical method, SPADE, SMIS, and our method. The detector can still recognize objects in our generated sample, while other images are too noisy. The depth estimation confirms the better quality of our generation by correctly estimating objects distances while producing blurred maps for comparisons.

methods often rely on small-scale networks with limited expressiveness and are therefore limited to a few scenarios. As a consequence, the potential applications of these methods are curtailed, preventing their widespread adoption in real-world situations where the complexity and variability of data are considerable.

A novel communication paradigm capable of preserving semantic information can be developed by exploiting the potential of deep generative models. Recently, denoising diffusion probabilistic models (DDPMs) [3] have exhibited remarkable achievements in a plethora of real-world generation tasks [4, 5, 6, 7]. Among such significant results, diffusion models are able to produce photorealistic images preserving the semantic layout [8, 9] in the so-called semantic image synthesis (SIS) task. The success of these models in countless domains, and especially in the SIS task, inspired us to involve them in semantic communication.

In this paper, we take a step towards bridging semantic communication and state-of-the-art generative models by presenting a novel generative semantic communication framework that meets the need for powerful models in semantic communication methods. The core of our framework is a semantic diffusion model that generates photorealistic images preserving the transmitted layout. The sender transmits the compressed semantic layout over the noisy channel. The corrupted information is collected by the receiver, which applies fast denoising to the maps before involving them in the generative process. We make the whole framework robust to bad channel conditions, ensuring that even in the case of extremely degraded received information, objects, their positions, and their depths are still recognizable in synthesized images, differently from existing approaches. Moreover, our framework can significantly compress the transmitted content without causing any information loss due to the transmission of binary maps. Through a detailed assessment of seven different channel conditions and two datasets, we demonstrate the ability of our framework to generate photorealistic images consistent with the transmitted semantic information even in the case of extremely corrupted received layouts. Furthermore, we show how the proposed method allows crucially reducing the information to transmit across the channel by involving binary maps only.

2 Related Works

Semantic communication is expected to play a key role in 6G networks [10, 1, 11, 12]. The core idea of this field is to focus on the meaning of the transmitted message, rather than on the full bit recovery. Indeed, bits may be directly affected by bad channel conditions, while the overall message may be preserved even in the case of syntactic mismatches. This novel view of wireless communication is influencing several applications ranging from image [13, 14], to video compression and transmission [15, 16], and it is expected to increase its impact in much more fields in the next years [2].

Diffusion models have brought a real breakthrough in generative modeling, showing impressive results in several generation tasks, ranging from image [17, 4, 5, 18] to audio [6, 19, 20, 21] or video generation [7, 22, 23, 24]. Diffusion models synthesize samples starting from a standard Gaussian distribution and by performing an iterative denoising process up to the desired new content. This process makes diffusion model generation far stabler than generative adversarial networks

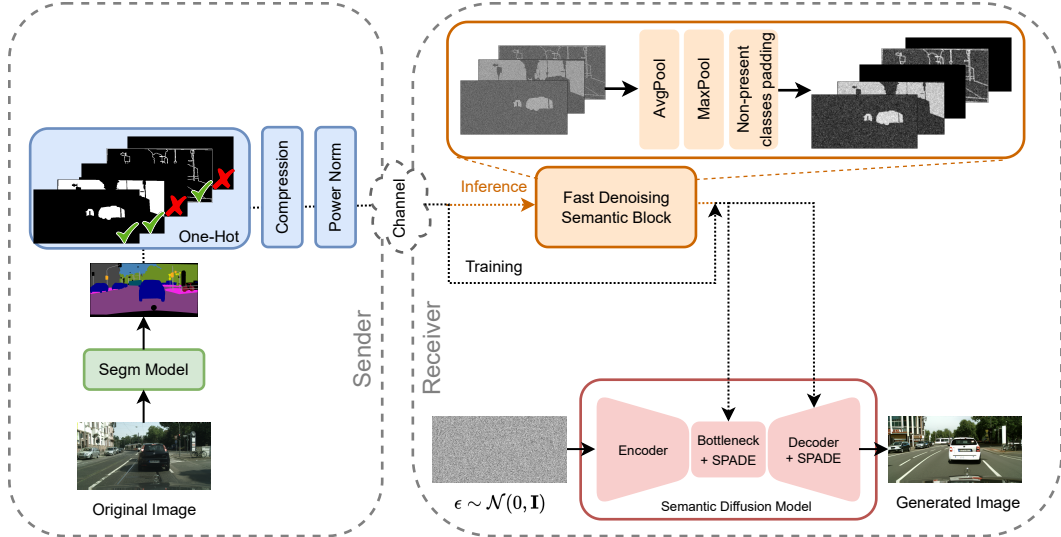


Figure 2: Proposed generative semantic communication framework. The sender transmits one-hot, compressed, and normalized encoded maps over the noisy channel. The receiver takes the noisy maps and directly involves them to train the semantic diffusion model. During inference, the receiver applies a fast denoising to the semantic information in order to improve image quality.

[25]. Among the tasks in which diffusion models stand out, there is semantic image synthesis (SIS), which is the task of generating images consistent with a given semantic layout. Although most SIS approaches is based on generative adversarial networks [26, 27, 28, 29, 30], in the last year, a novel SIS model surpasses other approaches by involving a diffusion model for synthesizing semantically-consistent high-quality scenes [8].

In recent months, generative semantic communication methods are coming into the world. Among them, generative adversarial networks have been the first generative tool to be involved in tasks such as image compression or denoising [31, 32]. Overall, existing generative communication frameworks are often limited to quite-simple models such as small VAEs [33, 34] or pretrained GAN generators [32]. In addition, normalizing flows have started to be involved in semantic communications to increase framework expressiveness [35]. However, there are often misleading definitions of semantics in such works, frequently mixing it up with the style, from which the semantics is instead usually disentangled [36]. Moreover, these networks have been often involved in tasks that underestimate their capabilities, limiting their effectiveness.

3 Proposed Method

In this paper, we present a novel generative semantic communication framework based on denoising diffusion probabilistic models (DDPMs) for synthesizing high-quality images that preserve the transmitted semantic information.

3.1 Problem Setting

Each communication method has to face the physical challenges imposed by real-world systems. First of all, the transmitter has to respect a power constraint on the transmitted signal \mathbf{z} in order to account for the limited transmit power of the sender device. This implies $1/k \mathbb{E}_{\mathbf{z}}[\|\mathbf{z}\|_2^2] \leq P$ [32]. Then, the signal flows over a noisy channel. To be consistent with the literature [32, 37], we consider the benchmark situation of additive white Gaussian noise (AWGN), where the noise ϵ is sampled from $\epsilon \sim \mathcal{N}(\mathbf{0}, \sigma^2 \mathbf{I})$, whereby σ^2 is the noise variance, and then added to the transmitted symbols as $\tilde{\mathbf{z}} = \mathbf{z} + \epsilon$. According to this formulation, the peak signal-to-noise ratio (PSNR) can be defined as

$$\text{PSNR} = 10 \log \frac{P}{\sigma^2} \text{ (dB)}. \quad (1)$$

In our simulations, we assume that the PSNR ranges from 0 to 100. For PSNR values close to 100 the channel has perfect conditions and the information flows without corruption, while for very low PSNR values ($\text{PSNR} \leq 20$) the noise can heavily corrupt the transmitted information, severely distorting the received content. Additionally, the communication channel bandwidth is usually limited and systems try to save as much bandwidth as possible to avoid bits loss or channel overload. Consequently, the transmitted information has to be significantly compressed, sometimes causing information loss. In this paper, we present a solution to address both of these communication problems, building a framework robust to any AWGN channel condition, and transmitting only extremely compressed content with negligible loss of information.

3.2 Generative Semantic Communication Framework

We introduce a novel generative semantic communication framework, whose core is a semantic diffusion model. Such a model generates high-quality images under the guidance of the semantic information brought by semantic maps. Figure 2 presents the proposed architecture including both sender and receiver sides.

Sender. To process the original image and generate a semantic map, any existing segmentation model can be used, as there is no need for communication between sender and receiver networks. Previous studies have demonstrated that conditioning a model with a one-hot encoded map yields better results compared to conditioning with a single segmentation map. For this reason, we adopt such an approach. However, transmitting the one-hot encoded information over a noisy channel may cause some issues. Indeed, empty contents corresponding to non-present classes become highly corrupted data, introducing significant noise into the resulting generated image. Furthermore, transmitting such content occupies valuable channel bandwidth with irrelevant information, further deteriorating the channel conditions.

To address these problems, we propose a solution that transmits only the most informative content. By doing so, we eliminate noisy-only information while maximizing the utilization of the available bandwidth. Once this procedure is complete, we apply a very strong compression of subject the encoded maps. This reduces the number of bits to be transmitted without sacrificing information, especially since, contrary to RGB images, the black-and-white regions of one-hot maps are minimally affected by strong compression methods, as we show in the supplementary material. Finally, we normalize features power P to 1 and transmit the semantic content.

Receiver. The core of the proposed method lies on the receiver side. The received one-hot maps are significantly corrupted from the communication channel making them extremely noisy. To make the diffusion model robust to such distorted content, we train it with such noisy maps and let the network weights adapt to different channel conditions. However, to improve the quality of generated images during inference, we insert a fast-denoising semantic (FDS) block, whose scope is to attenuate the random noisy condition of received maps. It is important to note that, differently from previous methods [37, 32], our receiver does not need to be aware of the channel conditions. Then, we sample $\mathbf{x}_0 \sim \mathcal{N}(\mathbf{0}, \mathbf{I})$ and we progressively remove noise up to synthesizing a new sample whose semantics reflects the conditioning one.

Fast Denoising Semantic Block. The fast-denoising semantic (FDS) block takes in input the heavily-corrupted one-hot encoded maps $\hat{\mathbf{y}}$ that have been transmitted over the noisy channel. FDS applies a fast denoise taking into account the black-and-white nature of the information. In detail, FDS produces the complete denoised semantic maps \mathbf{y} by:

$$\mathbf{y} = \text{Pad}(\text{MaxPool}(\text{AvgPool}(\hat{\mathbf{y}}))). \quad (2)$$

First, the average pooling removes noise spikes in the maps. Then, since the maps comprise large 0/1 regions, where 1 corresponds to areas where the class is present and 0 to empty spaces, the MaxPool performs a high-pass filter operation mainly keeping the 1s regions only and discarding other values. Finally, FDS pads the clean missing classes that have been removed on the sender side.

3.3 Semantic Diffusion Model

The core of our generative semantic communication framework is the semantic diffusion model that generates images by preserving the transmitted semantic information.

Conditional diffusion model. Given a sample \mathbf{x}_0 and a conditioning \mathbf{y} , the conditional data distribution follows $q(\mathbf{x}_0|\mathbf{y})$. In this setup, conditional diffusion models maximize the likelihood $p_\theta(\mathbf{x}_0|\mathbf{y})$. The reverse process is a Markov chain with learned Gaussian transitions that starts at $p(\mathbf{x}_T) \sim \mathcal{N}(0, \mathbf{I})$ and is defined as

$$p_\theta(\mathbf{x}_{0:T}|\mathbf{y}) = p(\mathbf{x}_T) \prod_{t=1}^T p_\theta(\mathbf{x}_{t-1}|\mathbf{x}_t, \mathbf{y}), \quad (3)$$

with $p_\theta(\mathbf{x}_{t-1}|\mathbf{x}_t, \mathbf{y}) = \mathcal{N}(\mathbf{x}_{t-1}; \mu(\mathbf{x}_t, \mathbf{y}, t), \sigma_\theta(\mathbf{x}_t, \mathbf{y}, t))$. The forward process $q(\mathbf{x}_{1:T}|\mathbf{x}_0)$ injects Gaussian noise into data following the defined variance schedule β_1, \dots, β_T . Considering that $\alpha_t := \prod_{s=1}^t (1 - \beta_s)$, the forward process is defined by

$$q(\mathbf{x}_t|\mathbf{x}_0) = \mathcal{N}(\mathbf{x}_t; \sqrt{\alpha_t}\mathbf{x}_0, (1 - \alpha_t)\mathbf{I}). \quad (4)$$

Encoder. The U-Net [38] encoder comprises an input convolution and a stack of encoder blocks with downsampling. The encoder block interleaves a convolution layer, a SiLU activation [39], and a group normalization [40]. The block also implements a fully-connected layer with weights \mathbf{w} and bias \mathbf{b} to inject the time information t by scaling and shifting the mid-activation \mathbf{a} by $\mathbf{a}_{i+1} = \mathbf{w}(t) \cdot \mathbf{a}_i + \mathbf{b}(t)$. Furthermore, at resolutions 32×32 , 16×16 , and 8×8 the encoder involves attention modules with skip connection. Given \mathbf{x} input and \mathbf{y} output of the attention block, and four 1×1 convolutions with weights $\mathbf{w}_f, \mathbf{w}_g, \mathbf{w}_h$, and \mathbf{w}_v , we define $f(\mathbf{x}) = \mathbf{w}_f\mathbf{x}$, $g(\mathbf{x}) = \mathbf{w}_g\mathbf{x}$ and $h(\mathbf{x}) = \mathbf{w}_h\mathbf{x}$, arriving to

$$\mathcal{M}(u, v) = \frac{f(\mathbf{x}_u)^\top g(\mathbf{x}_v)}{\|f(\mathbf{x}_u)\| \|g(\mathbf{x}_v)\|}, \quad (5)$$

$$\mathbf{y}_u = \mathbf{x}_u + \mathbf{w}_v \sum_v \text{softmax}_v(\alpha \mathcal{M}(u, v)) \cdot h(\mathbf{x}_v), \quad (6)$$

whereby the spatial dimension indexes are $u \in [1, H], v \in [1, W]$.

Decoder. The decoder blocks are crucial for the semantic conditioning of the whole model. Indeed, to fully exploit the semantic information, decoder blocks implement spatially-adaptive normalization (SPADE) [27] that replaces group normalization in the encoder. The SPADE module introduces semantic content in the data flow by adjusting the activations \mathbf{a}_i as follows

$$\mathbf{a}_{i+1} = \gamma_i(\mathbf{x}) \cdot \text{Norm}(\mathbf{a}_i) + \mathbf{b}_i(\mathbf{x}), \quad (7)$$

in which $\text{Norm}(\cdot)$ is the group normalization, and γ_i, \mathbf{b}_i are the spatially-adaptive weights and biases learned from the conditioning semantic map. It is worth noting that we train our semantic diffusion model directly with noisy semantic maps to let the network be robust to different channel noises. At each step, we simulate varying channel conditions by sampling the noise variance in $\{0.9, 0.6, 0.36, 0.22, 0.13, 0.05, 0.00\}$ corresponding to PSNRs in $\{1, 5, 10, 15, 20, 30, 100\}$, weighting perfect channel conditions (PSNR= 100) higher. We note that incorporating channel noise during training heavily impacts the quality of generated images in inference.

3.4 Loss Functions

We train the semantic diffusion model with a combination of two loss functions. Considering an input image \mathbf{x} and the sequence of time steps $t \in \{0, \dots, T\}$, the corresponding noisy image $\tilde{\mathbf{x}}$ at time t is built by $\tilde{\mathbf{x}} = \sqrt{\alpha_t}\mathbf{x} + \sqrt{1 - \alpha_t}\epsilon$. The noise is sampled from $\epsilon \sim \mathcal{N}(\mathbf{0}, \mathbf{I})$ and the α_t is the noise scheduler at t , where the maximum timestep is $T = 1000$. The model tries to predict the noise ϵ to reconstruct the reference image \mathbf{x} according to the guidance of the semantic map \mathbf{y} . The denoising loss function \mathcal{L}_d takes the form of

$$\mathcal{L}_d = \mathbb{E}_{t, \mathbf{x}, \epsilon} \left[\left\| \epsilon - \epsilon_\theta(\sqrt{\alpha_t}\mathbf{x} + \sqrt{1 - \alpha_t}\epsilon, \mathbf{y}, t) \right\|_2 \right]. \quad (8)$$

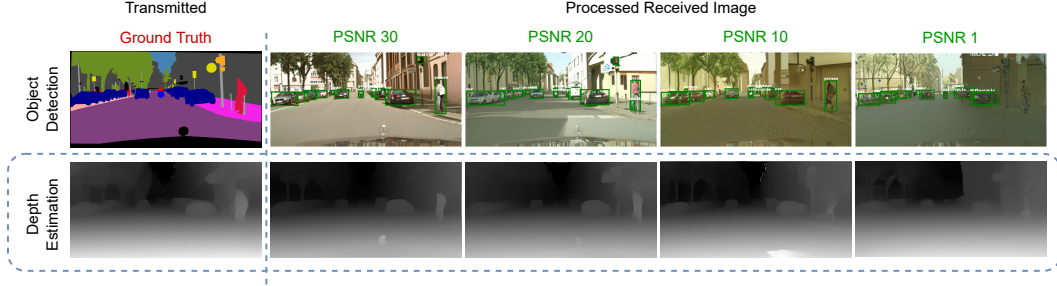


Figure 3: Our method results for different PSNR values of the communication channel. The detector recognizes well cars and pedestrians in all the samples, proving that our method works properly. Moreover, the depth estimation is consistent across all the scenarios, further validating the effectiveness of the proposed method.

In order to improve the generated images log-likelihood, the model is trained to predict variances too [41] by means of the KL divergence between the predicted distribution $p_\theta(\mathbf{x}_{t-1}|\mathbf{x}_t, \mathbf{y})$ and the diffusion process posterior $q(\mathbf{x}_{t-1}|\mathbf{x}_t, \mathbf{x}_0)$:

$$\mathcal{L}_{\text{KL}} = \text{KL}(p_\theta(\mathbf{x}_{t-1}|\mathbf{x}_t, \mathbf{y})||q(\mathbf{x}_{t-1}|\mathbf{x}_t, \mathbf{x}_0)). \quad (9)$$

The resulting loss function is balanced by λ as:

$$\mathcal{L} = \mathcal{L}_d + \lambda\mathcal{L}_{\text{KL}}. \quad (10)$$

3.5 Classifier-free Guidance

The image quality of conditional diffusion models can be improved through the gradient of the log-probability distribution $\nabla_{\mathbf{x}_t} \log p(\mathbf{y}|\mathbf{x}_t)$ by perturbing the mean with a guidance-scale hyperparameter s [42]. While previous diffusion models involved a classifier for this procedure [42], novel methods directly leverage the generative model power to provide the gradient during the sampling step [43]. In our framework, we can disentangle the conditional noise estimation from the unconditional one, by involving the semantic map for the first estimate as $\epsilon_\theta(\mathbf{x}_t|\mathbf{y})$ and the null label for the second one, that is $\epsilon_\theta(\mathbf{x}_t|\mathbf{0})$ [8]. The gradient of the log-probability distribution is then proportional to the difference between the estimates as

$$\epsilon_\theta(\mathbf{x}_t|\mathbf{y}) - \epsilon_\theta(\mathbf{x}_t|\mathbf{0}) \propto \nabla_{\mathbf{x}_t} \log p(\mathbf{x}_t|\mathbf{y}) - \nabla_{\mathbf{x}_t} \log p(\mathbf{x}_t) \quad (11)$$

$$\propto \nabla_{\mathbf{x}_t} \log p(\mathbf{y}|\mathbf{x}_t). \quad (12)$$

Accordingly, the noise estimation is performed by means of the disentangled component as

$$\hat{\epsilon}_\theta(\mathbf{x}_t|\mathbf{y}) = \epsilon_\theta(\mathbf{x}_t|\mathbf{y}) + s \cdot (\epsilon_\theta(\mathbf{x}_t|\mathbf{y}) - \epsilon_\theta(\mathbf{x}_t|\mathbf{0})). \quad (13)$$

4 Experimental Evaluation

In this Section, we report the experimental setup and the results of the tests we conduct.

4.1 Setup

Datasets. We involve Cityscapes, which contains 35 classes, and COCO-Stuff, with 183 classes, as our datasets for training and evaluation. Both these datasets comprise instance annotations that we consider in our framework.

Evaluation. The purpose of a semantic communication framework is to properly transmit the meaning of the image the sender wants to communicate to the receiver. Therefore, the crucial part of the



Figure 4: Comparisons among most performing models (CC-FPSE [30], OASIS [28], and SMIS [29]) with PSNR = 15. Other methods produce almost noise-only images. Our method produces the best quality samples in which it is easy to recognize objects, cars, and pedestrians, while comparisons generate scenes heavily corrupted by noise.

Table 1: Semantic evaluation of generated images under different channel conditions.

Method	mIoU \uparrow						
PSNR	100	30	20	15	10	5	1
Full image	-	0.955 \pm .032	0.911 \pm .155	0.906 \pm .247	0.906 \pm .339	0.240 \pm .193	0.110 \pm .298
SPADE [27]	0.909 \pm .127	0.914 \pm .255	0.921 \pm .315	0.812 \pm .364	0.672 \pm .321	0.253 \pm .288	0.313 \pm .144
CC-FPSE [30]	0.908 \pm .045	0.908 \pm .121	0.911 \pm .315	0.928 \pm .345	0.852 \pm .245	0.653 \pm .183	0.322 \pm .284
SMIS [29]	0.909 \pm .064	0.919 \pm .066	0.909 \pm .214	0.931 \pm .208	0.901 \pm .244	0.899 \pm .290	0.876 \pm .211
OASIS [28]	0.910 \pm .111	0.908 \pm .191	0.912 \pm .232	0.697 \pm .165	0.662 \pm .356	0.345 \pm .112	0.232 \pm .191
SDM [8]	0.921 \pm .051	0.340 \pm .022	0.333 \pm .061	0.351 \pm .011	0.297 \pm .021	0.256 \pm .019	0.211 \pm .043
Our method	0.940 \pm .014	0.942 \pm .212	0.944 \pm .297	0.945 \pm .141	0.905 \pm .112	0.913 \pm .214	0.925 \pm .111

evaluation is measuring the preserved semantic meaning in the synthesized images from the receiver. To this end, in addition to image quality evaluation with FID and LPIPS, we perform three different types of assessment. First, we compute and objectively evaluate the semantic interpretability of the generated images by building the semantic maps of the latter and comparing them with the original ones. We compute the mIoU metric on segmentation maps of generated images obtained through a pretrained model. For this evaluation, we employ DRN-D-105 [44] on Cityscapes, and MaskFormer [45] on COCO-Stuff. Note that the mIoU evaluation strongly depends on the effectiveness of the pretrained model involved to compute the segmentation maps. Second, we evaluate how much the synthesized images preserve objects meaning which is crucial for semantic communication systems in autonomous driving. As an example, buildings or landscapes can be badly generated as long as pedestrians or bicycles are well-recognized by the car. For this evaluation, we employ DETR [46]. Third, another key aspect of autonomous driving is depth estimation, which helps estimate the distance between objects [47], thus we evaluate this aspect via DPT [48].

Hyperparameters. The features dimension in the encoder and in the decoder of the U-Net model is halved at each layer, while comprising a number of channels equal to [256, 256, 512, 512, 1024, and 1024]. We involve attention blocks on the bottom 3 layers. We involve multi-head self-attention mechanism with a number of channels in each head equal to 64. For the diffusion process, we consider a $T = 1000$, and a linear variance schedule. Finally, we set the guidance scale s equal to 2 for Cityscapes and 2.5 for COCO-Stuff.

4.2 Comparisons and Results Analysis

We compare our proposal with classical communication methods that directly transmit the image over the channel. For more comparisons, we consider well-known semantic image synthesis models such as SPADE [27], CC-FPSE [30], SMIS [29], OASIS [28], and SDM [8]. We consider different channel scenarios, ranging from extremely degraded conditions to perfect transmissions, by setting PSNR values in $\{1, 5, 10, 15, 20, 30, 100\}$, and two datasets that are Cityscapes and COCO-Stuff.

Table 2: Perceptual similarity evaluation of generated images under different channel conditions.

Method	LPIPS↓						
	100	30	20	15	10	5	1
Full image	-	0.623±.074	0.684±.165	0.713±.054	0.730±.156	0.747±.154	0.738±.186
SPADE [27]	0.546 ±.045	0.565±.072	0.603±.022	0.726±.019	0.792±.115	0.824±.054	0.827±.011
CC-FPSE [30]	0.546 ±.025	0.559±.004	0.581±.009	0.620±.011	0.855±.024	0.753±.032	0.812±.055
SMIS [29]	0.546 ±.002	0.548±.030	0.561±.010	0.574±.021	0.603±.027	0.649±.044	0.680±.124
OASIS [28]	0.561±.032	0.564±.054	0.580±.012	0.613±.073	0.679±.020	0.783±.034	0.828±.122
SDM [8]	0.549±.061	0.543±.072	0.555±.066	0.599±.043	0.606±.071	0.655±.098	0.749±.119
Our method	0.606±.032	0.517 ±.004	0.523 ±.011	0.542 ±.003	0.549 ±.009	0.620 ±.023	0.609 ±.042

Table 3: Generation quality evaluation of generated images under different channel conditions.

Method	FID×10 ↓						
	100	30	20	15	10	5	1
Full image	-	6.284 ±.053	13.684±.032	20.045±.865	28.005±.878	37.931±.639	42.004±.911
SPADE [27]	10.324±.171	14.200±.179	22.971±.190	42.681±.201	55.420±1.056	noise	noise
CC-FPSE [30]	24.590±.056	20.337±.060	26.253±.049	33.166±.210	40.374±.345	noise	noise
SMIS [29]	8.758 ±.162	9.147±.100	11.750 ±.095	14.775±.129	21.373±.167	34.586±.171	44.115±.412
OASIS [28]	10.403±.053	10.339±.099	16.179±.122	24.892±.134	40.440±.349	noise	noise
SDM [8]	9.899±.391	16.642±2.101	31.510±2.926	noise	noise	noise	noise
Our method	11.848±.061	12.355±.090	14.030±.201	14.008 ±.251	14.851 ±.193	15.315 ±.349	15.989 ±.561

Advantages. Based on the achieved results, we can see how the proposed method clearly outperforms its competitors according to all the metrics used in our assessment. In particular, our approach is far more robust to bad channel conditions, still preserving semantics meanings with $\text{PSNR} \leq 10$ according to the mIoU metric, as Table 1 shows for the Cityscapes dataset. Moreover, it also generates more perceptually similar samples with respect to all the other comparisons, as measured by the LPIPS metric in Table 2. Indeed, in the context of communications, the lower the LPIPS between the original image and the synthesized one, the better the generation is since the two images are perceptually similar [31]. Few methods manage to synthesize meaningful images with very low PSNRs values and the sample quality deteriorated as the channel conditions worsen. On the contrary, as Table 3 reports, the FID of the proposed method samples is the lowest and quite stable across all the different scenarios, proving that the generation of our model is robust to every channel condition. Figure 1 reports generated samples with $\text{PSNR} = 10$ of the classical method, SPADE, SMIS, and the proposed method. Our sample is of better quality and its depth is much closer to the original one with respect to comparisons that produce noisy images and blurred depths. Additionally, Figure 3 shows generated samples or different channel scenarios and the detected objects by DETR. Even in the case of $\text{PSNR} = 1$, DETR still recognizes the largest part of the objects. Furthermore, the DPT depth estimation also gives consistent results across different conditions, with synthesized images at low PSNRs preserving the depths similar to the original image depth. As a further comparison for image quality, we show diverse samples in Figure 4, where our method is compared to the three best comparisons. Although CC-FPSE, OASIS, and SMIS produce better samples with respect to other models, our method clearly generated the best quality samples. Indeed, in our samples objects, cars, and pedestrians are clearly recognizable, whereas in other images they are blurred or noisy. On the COCO-Stuff dataset, most of the state-of-the-art approaches produce noisy samples, while our method still provides meaningful samples able to achieve good performance, as Table 4 shows.

Additionally, we compare the number of bits sent over the channel among our method and the classical one that transmits the full image. On the Cityscapes dataset with images resized to 256×512 , transmitting the full image requires 1464000 bits, while, on average, the proposed method just needs 119000 bits, with a reduction of 92%.

Limitations. Although our framework achieves excellent results in every scenario we test and outperforms existing solutions, clearly there is still a lot to do in assessing the performance of our method to more complex channel models. In this work, we considered a flat fading channel model corrupted by additive Gaussian noise. In practice, the channel may be frequency-selective and possibly time-varying. Nevertheless, we are confident that the proposed framework may be robust also to different kinds of distortions introduced by the channel, provided that in the training phase, these scenarios are properly taken into account. Furthermore, diffusion model sampling may require

Table 4: Semantic, perceptual similarity, and generation quality evaluation with fixed PSNR = 10 on the COCO-Stuff dataset. We test state-of-the-art models that released working checkpoints for this dataset and our method.

Method	mIoU \uparrow	LPIPS \downarrow	FID $\times 10\downarrow$
Full image	0.331 \pm .145	0.687 \pm .003	40.562 \pm 2.513
SPADE [27]	noise	noise	noise
CC-FPSE [30]	noise	noise	noise
SDM [8]	noise	noise	noise
Our method	0.365\pm.096	0.683\pm.011	36.664\pm1.527

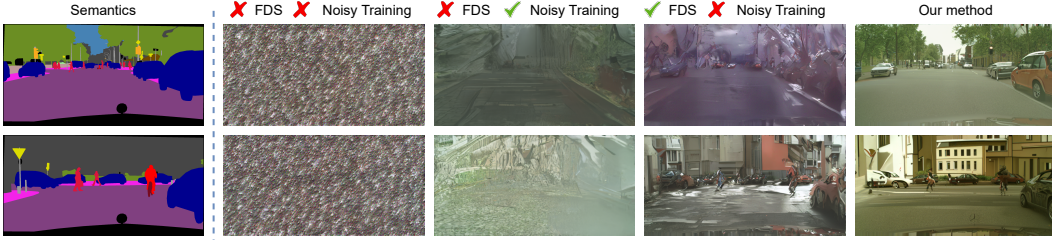


Figure 5: Generated samples from ablation studies with PSNR = 10. Samples without FDS and noisy training are clearly noisy. Then, both FDS and noisy training help improve samples quality up to the best quality achieved by our method.

a few seconds to generate a sample, therefore making this framework fit for offline applications or requiring improvements for online ones. We leave this aspect as a future research direction.

4.3 Ablation Studies

We perform ablation tests to corroborate our method choices. We study the inference performances with and without the proposed fast denoising semantic (FDS) block and without the noisy maps during training. We fix the PSNR to 10 and run the ablation on the Cityscapes dataset. Table 5 shows the effectiveness of the proposed choices for the framework and the importance of both the noisy training and the FDS module in inference. Figure 5 allows

Table 5: Ablation results on the Cityscapes dataset. Involving both the FDS module and the noisy training leads to the best results.

FDS	Noisy training	LPIPS	mIoU
\times	\times	noise	noise
\times	\checkmark	0.665	0.613
\checkmark	\times	0.663	0.713
\checkmark	\checkmark	0.549	0.905

for a visual inspection of the generated results without the proposed methods. While the semantic diffusion model alone (\times FDS \times Noisy Training) produces only noise, both FDS and the noisy training help to improve samples quality, up to the combination of the two methods leading to the best results.

5 Conclusion

To the best of our knowledge, this paper presents the first generative semantic communication framework whose core is a semantic diffusion model. In detail, we make the whole framework robust to bad channel conditions by training the semantic diffusion model with noisy semantics, and by inserting a fast denoising semantic block to improve inference image quality. Furthermore, we crucially reduce the amount of information to transmit by sending over the channel the present-classes binary maps only. Our performance assessment highlights that the proposed framework generates semantically-consistent samples even in the case of extremely degraded channel conditions, outperforming all other competitors.

References

- [1] X. Luo, H.-H. Chen, and Q. Guo, “Semantic communications: Overview, open issues, and future research directions,” *IEEE Wireless Comm.*, vol. 29, no. 1, pp. 210–219, 2022.
- [2] J. Dai, P. Zhang, K. Niu, S. Wang, Z. Si, and X. Qin, “Communication beyond transmitting bits: Semantics-guided source and channel coding,” *ArXiv preprint: ArXiv:2208.02481*, 2021.
- [3] J. Ho, A. Jain, and P. Abbeel, “Denoising diffusion probabilistic models,” in *Advances in Neural Information Processing Systems (NeurIPS)*, vol. 33, pp. 6840–6851, 2020.
- [4] C. Saharia, C. W., S. Saxena, L. Li, J. Whang, E. Denton, S. K. S. Ghasemipour, R. Gontijo-Lopes, B. K. Ayan, T. Salimans, J. Ho, D. J. Fleet, and M. Norouzi, “Photorealistic text-to-image diffusion models with deep language understanding,” in *Advances in Neural Information Processing Systems (NeurIPS)*, 2022.
- [5] R. Rombach, A. Blattmann, D. Lorenz, P. Esser, and B. Ommer, “High-resolution image synthesis with latent diffusion models,” in *IEEE/CVF Conference on Computer Vision and Pattern Recognition (CVPR)*, p. 10674–10685, 2021.
- [6] D. Ghosal, N. Majumder, A. Mehrish, and S. Poria, “Text-to-audio generation using instruction-tuned LLM and latent diffusion model,” *ArXiv preprint: ArXiv:2304.13731*, 2023.
- [7] W. Hong, M. Ding, W. Zheng, X. Liu, and J. Tang, “CogVideo: Large-scale pretraining for text-to-video generation via transformers,” in *International Conference on Learning Representations (ICLR)*, 2023.
- [8] W. Wang, J. Bao, W.-G. Zhou, D. Chen, D. Chen, L. Yuan, and H. Li, “Semantic image synthesis via diffusion models,” *ArXiv preprint: ArXiv:2207.00050*, 2022.
- [9] H. Xue, Z. H. Feng, Q. Sun, L. Song, and W. Zhang, “Freestyle layout-to-image synthesis,” *ArXiv preprint ArXiv:2303.14412*, 2023.
- [10] E. Calvanese Strinati and S. Barbarossa, “6G networks: Beyond Shannon towards semantic and goal-oriented communications,” *Computer Networks*, vol. 190, p. 107930, 2020.
- [11] J. Huang, D. Li, C. H. Xiu, X. Qin, and W. Zhang, “Joint task and data oriented semantic communications: A deep separate source-channel coding scheme,” *ArXiv preprint: ArXiv:2302.13580*, 2023.
- [12] Z. Qin, X. Tao, J. Lu, and G. Y. Li, “Semantic communications: Principles and challenges,” *ArXiv preprint: ArXiv:2201.01389*, 2021.
- [13] N. Patwa, N. A. Ahuja, S. Somayazulu, O. Tickoo, S. Varadarajan, and S. G. Koolagudi, “Semantic-preserving image compression,” *IEEE International Conference on Image Processing (ICIP)*, pp. 1281–1285, 2020.
- [14] C. Wang, Y. Han, and W. Wang, “An end-to-end deep learning image compression framework based on semantic analysis,” *Applied Sciences*, 2019.
- [15] P. Jiang, C.-K. Wen, S. Jin, and G. Y. Li, “Wireless semantic communications for video conferencing,” *IEEE Journal on Selected Areas in Communications*, vol. 41, pp. 230–244, 2022.
- [16] N. M. AL-Shakarji, F. Bunyak, H. Aliakbarpour, G. Seetharaman, and K. Palaniappan, “Performance evaluation of semantic video compression using multi-cue object detection,” in *IEEE Applied Imagery Pattern Recognition Workshop (AIPR)*, pp. 1–8, 2019.
- [17] A. Nichol, P. Dhariwal, A. Ramesh, P. Shyam, P. Mishkin, B. McGrew, I. Sutskever, and M. Chen, “GLIDE: Towards photorealistic image generation and editing with text-guided diffusion models,” in *International Conference on Machine Learning (ICML)*, 2021.
- [18] H. You, M. Guo, Z. Wang, K.-W. Chang, J. Baldridge, and J. Yu, “CoBIT: A contrastive bi-directional image-text generation model,” *ArXiv preprint: ArXiv:2303.13455*, 2023.
- [19] V. Popov, A. Amatov, M. Kudinov, V. Gogoryan, T. Sadekova, and I. Vovk, “Optimal transport in diffusion modeling for conversion tasks in audio domain,” in *IEEE International Conference on Acoustics, Speech and Signal Processing (ICASSP)*, pp. 1–5, 2023.
- [20] R. Huang, J.-B. Huang, D. Yang, Y. Ren, L. Liu, M. Li, Z. Ye, J. Liu, X. Yin, and Z. Zhao, “Make-An-Audio: Text-to-audio generation with prompt-enhanced diffusion models,” *ArXiv preprint: ArXiv:2301.12661*, 2023.

- [21] A. Turetzky, T. Michelson, Y. Adi, and S. Peleg, “Deep Audio Waveform Prior,” in *Interspeech*, pp. 2938–2942, 2022.
- [22] U. Singer, A. Polyak, T. Hayes, X. Yin, J. An, S. Zhang, Q. Hu, H. Yang, O. Ashual, O. Gafni, D. Parikh, S. Gupta, and Y. Taigman, “Make-A-Video: Text-to-video generation without text-video data,” *ArXiv preprint: ArXiv:2209.14792*, 2022.
- [23] X. Gu, C. Wen, J. Song, and Y. Gao, “Seer: Language instructed video prediction with latent diffusion models,” *ArXiv preprint: ArXiv:2303.14897*, 2023.
- [24] Y. Jiang, S. Yang, T. K. Liang, W. Wu, C. L. Change, and Z. Liu, “Text2Performer: Text-driven human video generation,” *ArXiv preprint: ArXiv:2304.08483*, 2023.
- [25] F.-A. Croitoru, V. Hondru, R. T. Ionescu, and M. Shah, “Diffusion models in vision: A survey,” *IEEE Transactions on Pattern Analysis and Machine Intelligence*, pp. 1–20, 2023.
- [26] Z. Tan, M. Chai, D. Chen, J. Liao, Q. Chu, B. Liu, G. Hua, and N. Yu, “Diverse semantic image synthesis via probability distribution modeling,” in *IEEE/CVF Conference on Computer Vision and Pattern Recognition (CVPR)*, pp. 7962–7971, 2021.
- [27] T. Park, M.-Y. Liu, T.-C. Wang, and J.-Y. Zhu, “Semantic image synthesis with spatially-adaptive normalization,” in *IEEE/CVF Conference on Computer Vision and Pattern Recognition (CVPR)*, 2019.
- [28] E. Schönfeld, V. Sushko, D. Zhang, J. Gall, B. Schiele, and A. Khoreva, “You only need adversarial supervision for semantic image synthesis,” in *International Conference on Learning Representations (ICLR)*, 2021.
- [29] Z. Zhu, Z.-L. Xu, A. You, and X. Bai, “Semantically multi-modal image synthesis,” *IEEE/CVF Conference on Computer Vision and Pattern Recognition (CVPR)*, pp. 5466–5475, 2020.
- [30] X. Liu, G. Yin, J. Shao, X. Wang, and H. Li, “Learning to predict layout-to-image conditional convolutions for semantic image synthesis,” in *Advances in Neural Information Processing Systems (NeurIPS)*, 2019.
- [31] T. Han, J. Tang, Q. Yang, Y. Duan, Z. Zhang, and Z. Shi, “Generative model based highly efficient semantic communication approach for image transmission,” *arXiv preprint: arXiv:2211.10287*, 2022.
- [32] E. Erdemir, T.-Y. Tung, P. L. Dragotti, and D. Gunduz, “Generative joint source-channel coding for semantic image transmission,” *arXiv preprint: arXiv:2211.13772*, 2022.
- [33] Y. Malur Saidutta, A. Abdi, and F. Fekri, “VAE for joint source-channel coding of distributed gaussian sources over AWGN MAC,” in *IEEE Int. Workshop on Signal Processing Advances in Wireless Comm. (SPAWC)*, pp. 1–5, 2020.
- [34] A. H. Estiri, M. R. Sabramooz, A. Banaei, A. H. Dehghan, B. Jamialahmadi, and M. J. Siavoshani, “A variational auto-encoder approach for image transmission in wireless channel,” *arXiv preprint: arXiv:2010.03967*, 2020.
- [35] T. Han, J. Tang, Q. Yang, Y. Duan, Z. Zhang, and Z. Shi, “Generative model based highly efficient semantic communication approach for image transmission,” *IEEE International Conference on Acoustics, Speech and Signal Processing (ICASSP)*, 2022.
- [36] X. Xu, Z. Wang, E. Zhang, K. Wang, and H. Shi, “Versatile diffusion: Text, images and variations all in one diffusion model,” *ArXiv preprint: ArXiv:2211.08332*, 2022.
- [37] J. Shao, Y. Mao, and J. Zhang, “Learning task-oriented communication for edge inference: An information bottleneck approach,” *IEEE Journal on Selected Areas in Communications*, vol. 40, pp. 197–211, 2021.
- [38] O. Ronneberger, P. Fischer, and T. Brox, “U-Net: Convolutional networks for biomedical image segmentation,” in *Medical Image Computing and Computer-Assisted Intervention (MICCAI)*, 2015.
- [39] P. Ramachandran, B. Zoph, and Q. V. Le, “Swish: a self-gated activation function,” *ArXiv preprint: ArXiv:1710.05941*, 2017.
- [40] Y. Wu and K. He, “Group normalization,” *International Journal of Computer Vision*, vol. 128, pp. 742–755, 2018.
- [41] A. Q. Nichol and P. Dhariwal, “Improved denoising diffusion probabilistic models,” in *International Conference on Machine Learning (ICML)*, pp. 8162–8171, 2021.

- [42] P. Dhariwal and A. Q. Nichol, “Diffusion models beat gans on image synthesis,” in *Advances in Neural Information Processing Systems (NeurIPS)*, vol. 34, 2021.
- [43] J. Ho and T. Salimans, “Classifier-free diffusion guidance,” in *Advances in Neural Information Processing Systems Workshops (NeurIPSW)*, 2021.
- [44] F. Yu, V. Koltun, and T. A. Funkhouser, “Dilated residual networks,” *IEEE/CVF Conference on Computer Vision and Pattern Recognition (CVPR)*, pp. 636–644, 2017.
- [45] B. Cheng, A. G. Schwing, and A. Kirillov, “Per-pixel classification is not all you need for semantic segmentation,” in *Neural Information Processing Systems*, 2021.
- [46] N. Carion, F. Massa, G. Synnaeve, N. Usunier, A. Kirillov, and S. Zagoruyko, “End-to-end object detection with transformers,” in *European Conference on Computer Vision (ECCV)*, pp. 213–229, 2020.
- [47] M. Fonder, D. Ernst, and M. Van Droogenbroeck, “M4Depth: Monocular depth estimation for autonomous vehicles in unseen environments,” *ArXiv preprint: ArXiv:2105.09847*, 2021.
- [48] R. Ranftl, A. Bochkovskiy, and V. Koltun, “Vision transformers for dense prediction,” *IEEE/CVF International Conference on Computer Vision (ICCV)*, pp. 12159–12168, 2021.
- [49] C. E. Shannon, “A mathematical theory of communication,” *The Bell system technical journal*, vol. 27, no. 3, pp. 379–423, 1948.
- [50] W. Weaver, “Recent contributions to the mathematical theory of communication,” *ETC: A Review of General Semantics*, pp. 261–281, 1953.

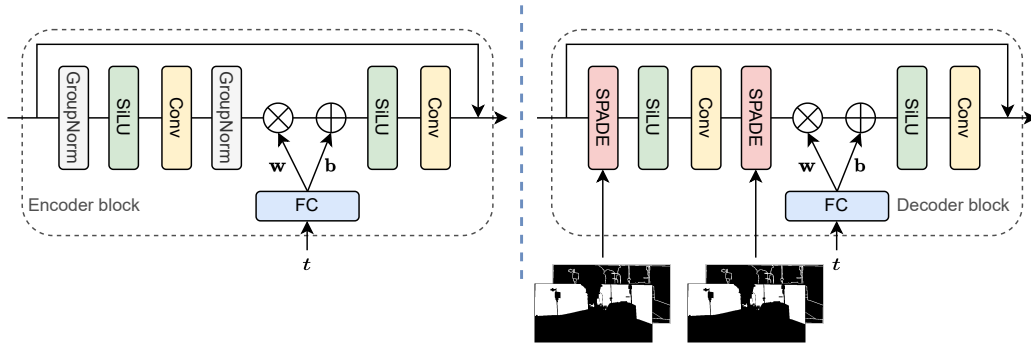


Figure 6: Encoder and decoder blocks of our U-Net-based semantic diffusion model.

Supplementary Material

From Technical to Semantic Communication Challenges

Since the channel capacity formula by Shannon in 1948 [49], communication systems have grown from first-generation (1G) to Beyond-fifth generation (B5G), progressively approaching the non-physical-layer capacity limit and designing new frontiers in line with users’ needs. In 1953, Weaver theorized that communication challenges can be enclosed in three gradual levels [50]:

1. **The technical challenge.** It deals with the classical Shannon’s communication theory and focuses on the proper way of transmitting bits from a sender to a receiver.
2. **The semantic challenge.** Rather than just transmitting bits, this level should account for properly transmitting the meaning of the messages the sender wants to communicate to the receiver.
3. **The effectiveness challenge.** This level deals with the efficiency of the transmission of previous levels.

With the upcoming advent of the sixth generation (6G), a radical rethinking of communication framework design has started, sliding from the first to the second level of Weaver’s theory [10, 1]. In this switch, generative learning methods are making their way bringing considerable improvements in several communication tasks, such as content compression or denoising [31, 32]. However, generative communication frameworks are often limited to quite-simple models such as small VAEs [33, 34] or pretrained GAN generators [32]. Moreover, these networks have been involved in tasks that underestimate their capabilities, limiting their effectiveness. On the contrary, the enormous power of recent generative models may lead to profoundly transform semantic communications.

Experimental Details

We provide additional details to reproduce our experiments. We resize Cityscapes images to 256×512 , and COCO-Stuff images to 256×256 . We train the model with PyTorch on a single NVIDIA Tesla V100 GPU (32GB) for the Cityscapes and on a single NVIDIA Quadro RTX8000 (48GB) for COCO-Stuff. We use a batch size of 4 in all the experiments, a learning rate of 0.0001 for the AdamW optimizer, and attention blocks at resolutions 32, 16, and 8 with a number of head channels equal to 64. The number of filters in the blocks is set to [256, 256, 512, 512, 1024, and 1024]. For sampling, we set the number of diffusion steps to $T = 1000$ with a linear noise schedule. We use mixed precision for training in order to reduce the computational complexity. The loss balance term λ is set to 0.001, according to [8]. Furthermore, we involve an exponential moving average of the U-Net network weights with a decay equal to 0.9999. Figure 6 shows the structure of our encoder and decoder blocks. The code and the checkpoints will be freely available at the end of the revision process.



Figure 7: Example of how the JPEG compression affects the original image and a sample of the one-hot encoded maps. The compressed image loses informative content, while the one-hot encoded maps are minimally affected by the compression.

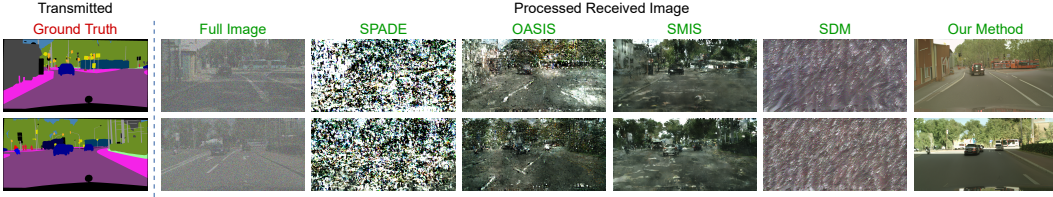


Figure 8: Other comparisons for transmitted semantics and a fixed PSNR value of 10.

Additional Experimental Results

Image vs Binary map transmission. In order to validate the claims of the main paper regarding maps compression, we show an example in Fig.7. The JPEG compression drastically reduces the informative content of the image. On the contrary, when applied to one-hot encoded binary maps, the content remains almost unchanged. For this reason, we can apply an aggressive compression algorithm to the transmitted maps in order to reduce the number of transmitted bits.

Further comparisons. Figure 8 provides additional comparisons for a given semantics under fixed channel conditions equal to $\text{PSNR} = 10$. While most of the samples generated from existing methods are heavily corrupted by noise, our method provides clearer images, while better preserving semantic features.

Generated samples from our model. We report additional examples of our method generation. We randomly select three semantics and then report the generated samples from our method with seven different PSNRs values. Results are shown in Fig. 9. Our method is able to generate good quality images even in the case of extremely degraded channel conditions corresponding to PSNR values equal to 5 and 1. Indeed, objects and positions are still evident in these scenarios too.

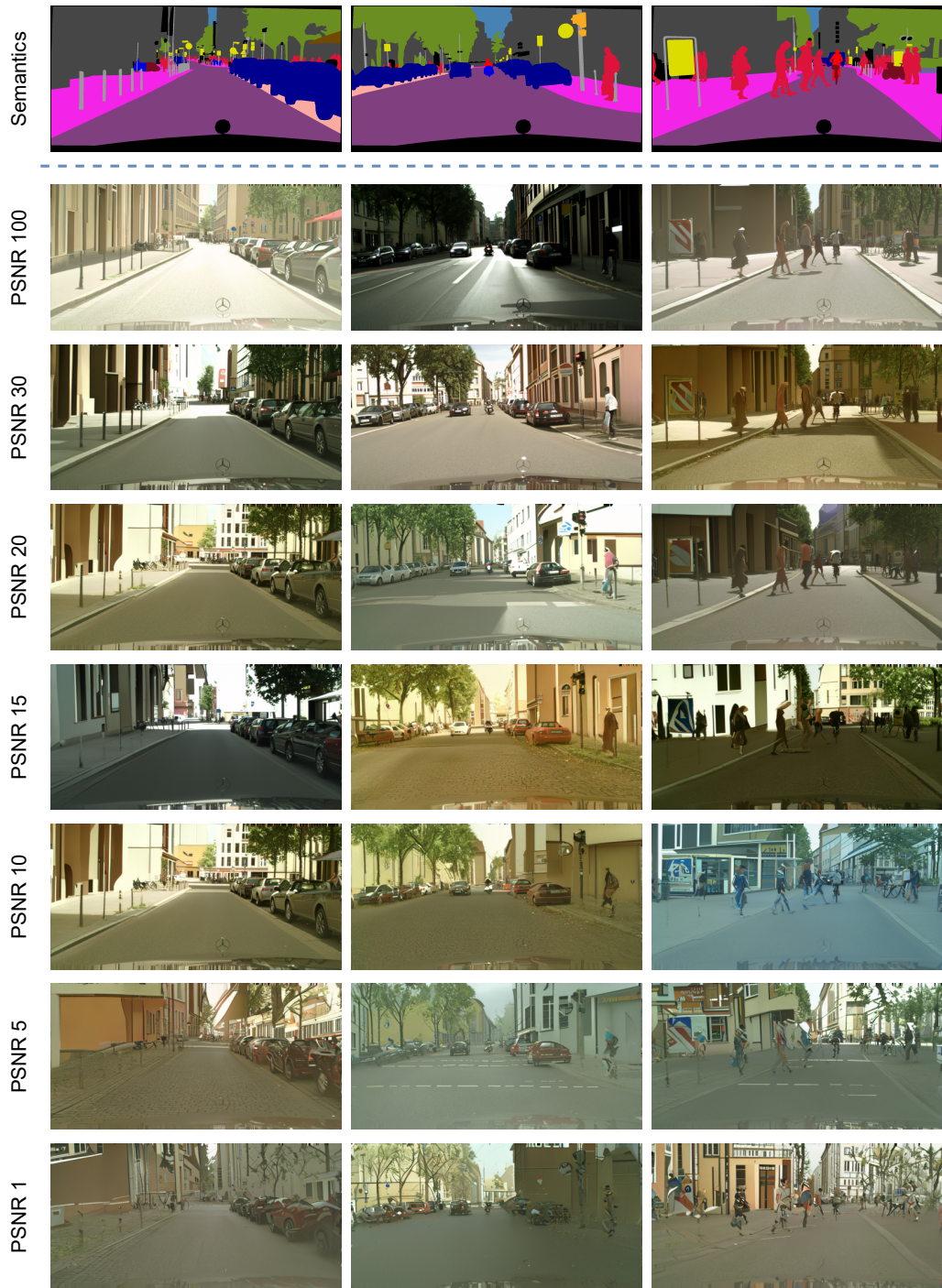


Figure 9: Generated samples of our method from the transmitted semantics under different PSNR values for simulating various channel conditions.